

# Restoration of Conductivity with TTF-TCNQ Charge-Transfer Salts

By Susan A. Odom, Mary M. Caruso, Aaron D. Finke, Alex M. Prokup, Joshua A. Ritchey, John H. Leonard, Scott R. White, Nancy R. Sottos, and Jeffrey S. Moore\*

The formation of the conductive TTF-TCNQ (tetrathiafulvalene–tetracyanoquinodimethane) charge-transfer salt via rupture of microencapsulated solutions of its individual components is reported. Solutions of TTF and TCNQ in various solvents are separately incorporated into poly(urea-formaldehyde) core–shell microcapsules. Rupture of a mixture of TTF-containing microcapsules and TCNQ-containing microcapsules results in the formation of the crystalline salt, as verified by FTIR spectroscopy and powder X-ray diffraction. Preliminary measurements demonstrate the partial restoration of conductivity of severed gold electrodes in the presence of TTF-TCNQ derived in situ. This is the first microcapsule system for the restoration of conductivity in mechanically damaged electronic devices in which the repairing agent is not conductive until its release.

## 1. Introduction

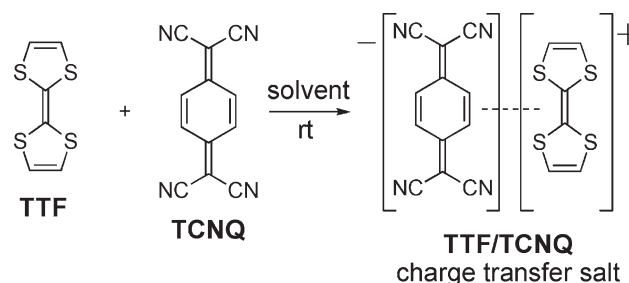
Mechanical durability is an important concern for integrated microelectronic devices.<sup>[1–4]</sup> Thermomechanical failures result from the mismatch of thermal expansion coefficients, Young's modulus, and Poisson's ratio of the package materials.<sup>[5]</sup> These mismatches are the most common reasons for failures in integrated circuits that are caused by discontinuities, or “electrical opens.”<sup>[6]</sup> Despite the importance of mechanical failures to the lifetime of electronic circuitry, the development of electronic devices that are capable of autonomously repairing mechanical damage in electronic devices remains a relatively unexplored

strategy.<sup>[7–9]</sup> One of the few attempts to demonstrate electronic self-healing was reported by Bielawski and co-workers in the examination of reversible bond formation between *N*-heterocyclic carbenes and transition metals.<sup>[7]</sup>

The development of electronic devices capable of autonomic repair requires self-healing components that are transported to the site of damage and subsequently activated. Self-healing polymers<sup>[10–13]</sup> that utilize microencapsulated polymer precursors or reagents and efficiently heal damage from external stimuli are excellent examples that display requisite mass transport and activation behavior. Recently, Caruso et al. encapsulated suspensions of conduc-

tive carbon nanotubes in the core of poly(urea-formaldehyde) (PUF) microcapsules and successfully released the nanotubes upon capsule rupture.<sup>[9]</sup> For the present study, we explore an approach in which the conductive healing agent is generated upon mechanical damage. The major advantage of this approach is the greater mobility of the precursor solutions compared to suspensions of conductive particles; here it is possible that both core solutions may travel by capillary action to the relevant damage site before forming the conductive salt.

The conductive tetrathiafulvalene–tetracyanoquinodimethane (TTF-TCNQ) charge-transfer salt<sup>[14,15]</sup> is a promising system for restoration of conductivity that can be generated from solutions of its precursors. Individually, TTF and TCNQ are soluble in a variety of organic solvents, commercially available in bulk quantity, and are non-conductive. The formation of the relatively insoluble charge-transfer salt (Scheme 1) occurs rapidly at room temperature,



Scheme 1. Formation of TTF/TCNQ charge-transfer salt.

[\*] Prof. J. S. Moore, Dr. S. A. Odom, M. M. Caruso, A. D. Finke, A. M. Prokup, J. A. Ritchey, J. H. Leonard  
Department of Chemistry and The Beckman Institute  
University of Illinois at Urbana-Champaign  
405 N. Mathews Ave. Urbana, IL 61801 (USA)  
E-mail: jsmoore@uiuc.edu

Prof. N. R. Sottos  
Department of Materials Science & Engineering and  
The Beckman Institute  
University of Illinois at Urbana-Champaign  
405 N. Mathews Ave. Urbana, IL 61801 (USA)

Prof. S. R. White  
Department of Aerospace Engineering and The Beckman Institute  
University of Illinois at Urbana-Champaign  
405 N. Mathews Ave. Urbana, IL 61801 (USA)

DOI: 10.1002/adfm.201000159

and preferentially forms the TTF-TCNQ salt in a 1:1 molar ratio, even when TTF and TCNQ are not combined in equal amounts.<sup>[16]</sup> Rapid and spontaneous generation of conductive TTF-TCNQ via microcapsule delivery of solutions of its constituents could enable autonomous conductivity restoration.

Single-crystal TTF-TCNQ shows a high conductivity of ca.  $400\text{--}500\text{ S}\cdot\text{cm}^{-1}$ ,<sup>[17,18]</sup> making it a useful material for electronic devices.<sup>[19–21]</sup> The conductivity of polycrystalline TTF-TCNQ has also been investigated, fabricated through chemical vapor deposition,<sup>[22]</sup> thermal evaporation,<sup>[23]</sup> and from crystals grown from combined solutions of TTF (the electron donor) and TCNQ (the electron acceptor).<sup>[24]</sup> These films generally have conductivities of  $5\text{--}30\text{ S}\cdot\text{cm}^{-1}$ .<sup>[19,22,25]</sup> In a recent example of solution-based salt formation, conductive films and circuits were deposited onto substrates using inkjet printing of the donor and acceptor solutions, forming the charge-transfer salt (in ca. 10 s) before complete solvent (dimethyl sulfoxide) evaporation. Without post-process annealing, this method produced films with conductivities of  $5\text{--}10\text{ S}\cdot\text{cm}^{-1}$ ,<sup>[24]</sup> comparable to that of vacuum-deposited films.<sup>[19,22,25]</sup>

In this article, we report the encapsulation of individual solutions of TTF and TCNQ, as well as characterization of the core materials. We additionally demonstrate the formation of the TTF-TCNQ charge-transfer salt from the rupture of a mixture of TTF- and TCNQ-containing microcapsules. We analyze the microcapsules upon rupture and report the electrical characterization of ruptured microcapsules to determine their potential for the restoration of electrical conductivity. These measurements include current–voltage ( $I\text{--}V$ ) sweeps of the microcapsules between tungsten probe tips and over severed gold circuits.

## 2. Results and Discussion

Unlike the straightforward encapsulation of conductive carbon nanotubes,<sup>[8]</sup> suspensions of the TTF-TCNQ salt were not readily encapsulated using an emulsification polymerization procedure. In a preliminary attempt to encapsulate polycrystalline TTF-TCNQ, we found that the crystals, regardless of size, were not incorporated within the microcapsules (abbreviated MCs in figures and tables) but instead adhere to the shell wall or are in partial contact with the microcapsule exterior (Fig. 1A). These resulting capsules, which contained a solvent core, collapsed upon drying and sieving. In a second approach, powdered TTF-TCNQ salt was encapsulated when the particle size was much smaller than the microcapsule diameter (Fig. 1B); however, microcapsules ruptured by manual crushing by mortar and pestle (the technique used for rupturing microcapsules throughout this publication) did not release the salt from the interior of the capsules (Fig. 1B, inset). Due to the difficulty of encapsulating the TTF-TCNQ salt directly, we investigated the encapsulation of individual solutions of each compound.

TTF and TCNQ were qualitatively screened in various solvents that have been shown to form high-quality microcapsules and promote self-healing in epoxy polymers.<sup>[26,27]</sup> While TTF displayed good solubility in most solvents, the solubility of TCNQ was much lower and proved to be the limiting factor in solvent choice. Of the solvents investigated, chlorobenzene (PhCl), ethyl phenylacetate (EPA), and phenyl acetate (PA) dissolved TCNQ significantly

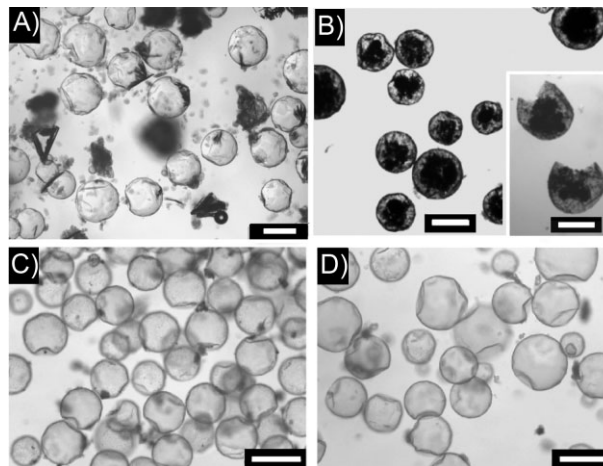


**Figure 1.** Optical microscope images from A) an attempt to encapsulate crystalline TTF-TCNQ salt in PA, B) MCs containing powdered TTF-TCNQ salt suspended in PA; inset: ruptured MCs containing powdered TTF-TCNQ salt in PA, C) TTF-PA MCs, and D) TCNQ-PA MCs. All scale bars are 200  $\mu\text{m}$ .

more than other encapsulatable solvents. The solubility of each compound and the minimum solution concentrations required for precipitation of the charge-transfer salt from mixed solutions of equal volumes and concentrations were determined for each solvent (Table S1). The minimum concentration required for salt precipitation for all solvents was one-half to one-third of the maximum solubility of TCNQ. For this test the minimum concentration required for precipitation was given for precipitation of the salt within 5 min after mixing room temperature solutions and the salt formed in all cases.

TTF and TCNQ were individually incorporated into microcapsule cores as solutions in PhCl, EPA, and PA at the maximum solution concentrations, although TCNQ suspensions were sonicated at  $40\text{ }^\circ\text{C}$  to allow for higher concentrations of TCNQ into the core solutions (Table S2). PUF core–shell microcapsules were prepared using an in situ emulsification polymerization following our reported procedure.<sup>[26,28]</sup> Higher concentrations of TTF and TCNQ were encapsulated in PA by modifying the encapsulation procedure through addition of 3.0 g of a polyurethane prepolymer to the core solution prior to addition to the reaction mixture.<sup>[29]</sup> Scanning electron microscope (SEM) and optical microscope images confirm microcapsule formation for all three solvent systems (Fig. 1C and D, and Supporting Information).

Electron impact mass spectra of the dried microcapsule core solutions confirmed the presence of TTF and TCNQ in the microcapsules (Fig. S8 and S9). Quantitative analysis of TTF and TCNQ was performed by taking the absorption spectra of diluted solutions of the microcapsule cores (Fig. 2). Beer's law plots of TTF and TCNQ in solvent provided quantitative calibration (see Supporting Information). The wt% of each compound was then calculated after correcting for solvent dilution based on spectra of the microcapsule core solutions (Table 1).

The amount of TTF in each type of microcapsule (by wt%) was similar to that of the initial core solutions. Sulfur elemental analysis of the isolated shell walls showed 1%–2% sulfur by mass,

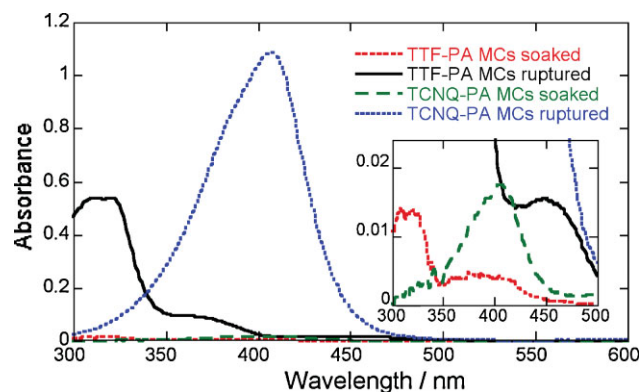


**Figure 2.** UV-vis absorption spectra of filtered suspensions of ruptured TTF-PA MCs (black), supernatant of TTF-PA MCs soaked for 60 min in PA (red), ruptured TCNQ-PA MCs (blue), and supernatant of TCNQ-PA MCs soaked for 60 min in PA (green), all spectra obtained from samples containing 2.0 mg MCs per mL PA.

**Table 1.** Weight percentages of TTF and TCNQ incorporated into the microcapsules based on UV-vis absorption spectra of diluted solutions of crushed, filtered microcapsules.

core solvent	TTF [wt%]	TCNQ [wt%]
PhCl	0.22	0.043
EPA	0.27	0.044
PA	0.75	0.34
PA [a]	1.1	0.70

[a] Polyurethane prepolymer added to microcapsule core.

which corresponds to 0.6–1.2 wt% TTF in the shell wall (Table S5). In all three solvents, the wt% of TCNQ in the microcapsule cores was significantly lower than the initial amount in the core solution. It is possible that TCNQ is incorporated into the shell wall or precipitated from solution, given its lower solubility in PA, resulting in the lower relative core concentrations. Consistent with this possibility for shell-wall incorporation is the green color of the TCNQ-PA microcapsule shell walls, presumably due to the presence of reduced TCNQ.<sup>[30]</sup> Importantly, the core solutions for TCNQ-PA (and TTF-PA) capsules are yellow, which is evident upon filtration of ruptured microcapsules.

Despite the relatively minor difference in solubilities of TTF and TCNQ in the three core solvents, the amounts of each compound incorporated into the microcapsule cores were ca. 3× higher and 10× higher (by wt%), respectively, for PA microcapsules than for PhCl and EPA microcapsules. In PA, the amount of TCNQ encapsulated was ca. 50% that of TTF. Attempts to increase the amount of encapsulated TCNQ by increasing the concentration of TCNQ in the core solvent by preparing supersaturated core solutions led to poor quality capsules that leached core content rapidly. PA microcapsules with higher concentrations of TTF or TCNQ were prepared with polyurethane prepolymer added to the core. The modified capsules showed increased thermally stability compared to the TTF-PA microcapsules (as measured by thermogravimetric analysis (TGA), see Supporting Information), but also showed significant leaching of core content after 2 weeks.

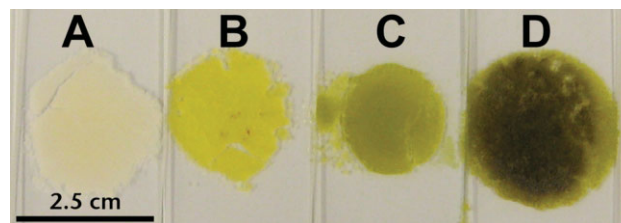


**Figure 3.** Microcapsules crushed between two glass slides: A) 50 mg PA-MCs; B) 50 mg TTF-PA MCs; C) 50 mg TCNQ-PA MCs; D) 50 mg each TTF-PA and TCNQ-PA MCs.

When mixtures of TTF and TCNQ microcapsules were ruptured, a dark-brown color was immediately observed, indicative of the TTF-TCNQ charge-transfer salt formation (Fig. 3). Previously, the TTF-TCNQ charge-transfer salt has been characterized by UV-vis-NIR absorption spectra in acetonitrile.<sup>[31]</sup> In this study, UV-vis analysis was not useful for determining of the formation of the TTF-TCNQ salt; the characteristic bands of the TCNQ radical anion (including one band with  $\lambda_{\text{max}}$  at 744 nm) that are used to identify the charge-transfer salt formation were present in the absorption spectrum of TCNQ in PA alone. This effect is presumably due to the electronic interaction of TCNQ with PA (see Supporting Information and Fig. S14 and S15 for more details).

Because UV-vis analysis was insufficient to determine the formation of the TTF-TCNQ salt, IR spectroscopy was used to verify charge-transfer salt formation. The C–H stretching region (Fig. 4) and C–N stretching region (Fig. S16) of neat TTF (3102, 3081, 3063  $\text{cm}^{-1}$ ), TCNQ (3050, 2220  $\text{cm}^{-1}$ ), and TTF-TCNQ (3093, 3073, 2203  $\text{cm}^{-1}$ ) were compared to spectra of the isolated core materials. In all three cases, the spectra of the core materials matched those of the neat compounds, consistent with incorporation of TTF and TCNQ into the microcapsules, as well as TTF-TCNQ salt formation upon microcapsule rupture and mixing.

When a mixture of ruptured TTF-PA and TCNQ-PA microcapsules was dispersed in mineral oil immediately after rupture and suspension in oil, optical micrographs revealed small particles that are not present in ruptured TTF-PA or TCNQ-PA microcapsules alone (Fig. 5 and S5). Powder X-ray diffraction (XRD) was

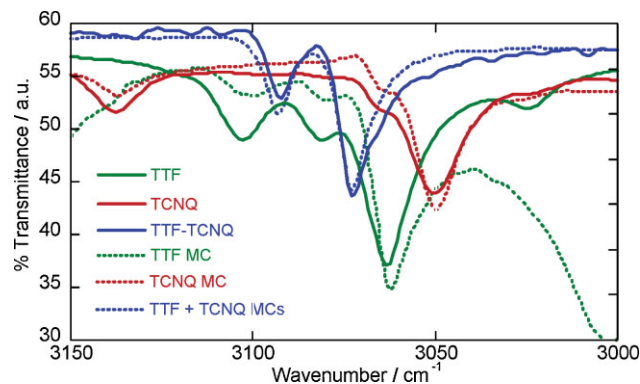


**Figure 4.** Selected region of the IR spectra of KBr pellets of TTF, TCNQ, and TTF-TCNQ (solid lines) and spectra from ruptured, filtered, and dried PA-based MCs (dotted lines).

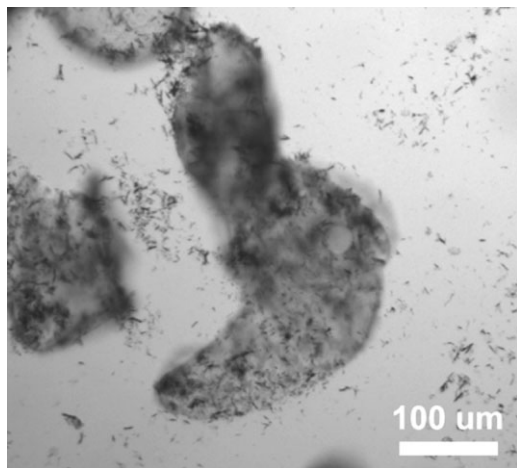


**Figure 5.** Optical micrograph of 1:1 (wt%) of crushed of TTF-PA:TCNQ-PA microcapsules dispersed in mineral oil.

used to determine if the particles were crystalline TTF-TCNQ. Because the presence of shell wall and polymer results in broad diffraction bands that interfere with the analysis of the precipitate itself, for this experiment, TTF-PA and TCNQ-PA microcapsules were individually ruptured and shell walls removed with a syringe filter; then a 1:1 v/v ratio of the cores was combined. A black solid immediately precipitated, which was filtered and washed with acetonitrile. Powder XRD analysis of the black solid gave a pattern that matched a simulated powder pattern based on the previously reported single crystal structure of TTF-TCNQ (Fig. 6 and Supporting Information), thus indicating the production of crystalline TTF-TCNQ.

After verifying the charge-transfer salt formed upon rupture and combination of TTF-PA and TCNQ-PA microcapsule cores, electrical properties of the ruptured microcapsules were examined by  $I$ - $V$  measurements. Before analyzing ruptured microcapsules, comparative solutions of TTF in PA, another of TCNQ in PA, and a suspension of TTF-TCNQ in PA were analyzed by a procedure for collecting  $I$ - $V$  data similar to that used for the analysis of microcapsules containing carbon nanotube suspensions.<sup>[8]</sup> For each case, the analyte was deposited onto a glass slide and two tungsten probe tips were immersed in the suspension, spaced approximately 100  $\mu\text{m}$  apart. The potential was varied from  $-10$  to  $+10$  V and the current was recorded. TTF in PA alone showed little measurable response to applied voltage, while TCNQ in PA and TTF-TCNQ in PA showed linear  $I$ - $V$  responses, with the  $I$ - $V$  ratio of TTF-TCNQ being more intense than that of TCNQ (Fig. S21a). It is possible that TCNQ in PA shows a  $I$ - $V$  response due to partial reduction upon interaction with PA. Measurements of TTF-TCNQ in PA at multiple concentrations were also recorded (Fig. S21b); the intensity of the response was dependent on the concentration of TTF-TCNQ. Observation by optical microscopy revealed that the TTF-TCNQ crystals aligned between the probe tips, similar to the behavior observed for carbon nanotube suspensions.<sup>[8]</sup>

The same measurements were performed for suspensions of crushed TTF-PA and TCNQ-PA microcapsules in a 1:1 ratio (wt%) at multiple concentrations in PA (Fig. 7a). The  $I$ - $V$  response was also linear for these cases and dependent on microcapsule wt%.

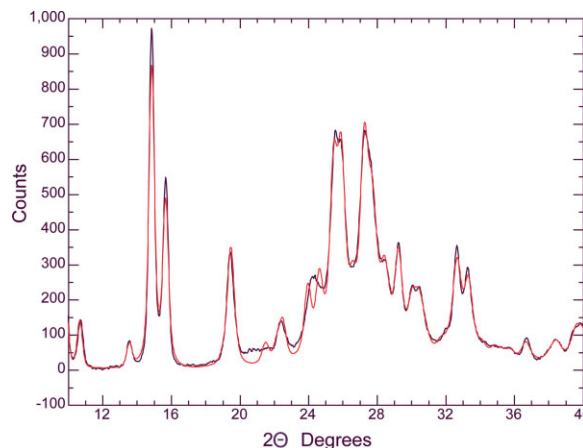


**Figure 6.** Experimentally observed diffraction pattern of the precipitate isolated from combining the TTF-PA and TCNQ-PA core materials (black) and simulated pattern (red).

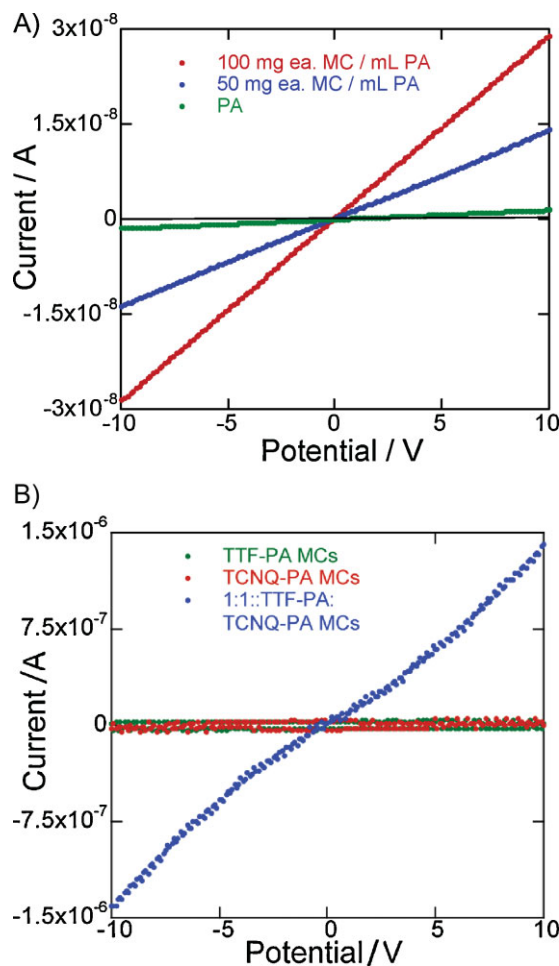


**Figure 7.**  $I$ - $V$  measurements of analytes on glass slides measured between two tungsten probe tips spaced approximately 100  $\mu\text{m}$  apart for A) PA and suspensions of ruptured TTF-PA and TCNQ-PA microcapsules in a 1:1 ratio (wt%) in PA, and B) neat ruptured TTF-PA, TCNQ-PA, and TTF-PA:TCNQ-PA in a 1:1 ratio (wt%) microcapsules.

*I*-*V* measurements were also obtained for neat ruptured TTF-PA and TCNQ-PA microcapsules, both individually and combined (Fig. 7b). In these measurements, the current reached a maximum value for the combination of TTF-PA and TCNQ-PA microcapsules after 5–7 scans, potentially due to increased alignment of the charge-transfer salt in subsequent scans (data is shown for the last scan). This phenomenon was previously observed in related work when suspensions of ruptured microcapsules containing carbon nanotubes were analyzed.<sup>[8]</sup> Without dilution, the neat ruptured microcapsule samples were too opaque to see individual crystals/particles and prevented optical confirmation of this effect.

The optimal ratio of TTF-PA:TCNQ-PA microcapsules for the restoration of conductivity was determined from *I*-*V* measurements performed on substrates containing model damage of an electrical circuit. Well-defined gap distances ( $\leq 100\ \mu\text{m}$ ) in conductive lines were fabricated using standard photolithography techniques and patterned masks. Gold lines were deposited onto glass slides with gaps of varying distances at the center of each line (30, 50, and  $100\ \mu\text{m}$ ), including one gold line with no gap as a control (Fig. 8, right). To ensure that the gaps were bridged with a consistent sample, an excess of ruptured microcapsules was deposited onto the substrate over the gaps in the gold lines. Tungsten probe tips were used to make contact with the gold lines, and the *I*-*V* response was measured (see image of the set-up in Fig. 8, left).

Initially, gold lines with  $50\ \mu\text{m}$  gaps were used to compare neat crushed microcapsules. The ratios of TTF-PA:TCNQ-PA microcapsules were varied to determine which combination of microcapsules gave the largest *I*-*V* response (Fig. 9a). The TTF-PA and TCNQ-PA microcapsules alone were also analyzed and showed no measurable current. Of the ratios of TTF-PA:TCNQ-PA microcapsules analyzed, the largest current response occurred with a 1:2 ratio. This ratio of capsules is consistent with delivering the optimal 1:1 ratio (by mass and molarity) of TTF:TCNQ, which is expected to yield the highest concentration of charge-transfer salt.

Once the ideal ratio of microcapsules was determined, this optimized ratio was used to examine the change in *I*-*V* response over multiple gap sizes to determine the potential for conductivity restoration for various damage states. In these experiments, a 1:2 ratio of neat crushed TTF-PA:TCNQ-PA microcapsules was applied to substrates over the 30, 50, and  $100\ \mu\text{m}$  gaps. As expected for a polycrystalline material, the *I*-*V* responses were larger for shorter gaps (Fig. 9b). All gap sizes showed conductivity restoration, indicating that the TTF-TCNQ charge-transfer salt bridges at least  $100\ \mu\text{m}$  distances upon microcapsule rupture.

Lastly, we examined the effect of solvent removal on the restoration of conductivity. To achieve a successful autonomic system, conductivity restoration must be maintained upon solvent evaporation. For this experiment, neat ruptured microcapsules were used to bridge the  $30\ \mu\text{m}$  gap. Cycling was performed until the maximum *I*-*V* was obtained (5–7 scans). The microcapsules were then allowed to air dry on the substrate. After drying, *I*-*V* scans were performed on the same substrate. For the dried microcapsules, the *I*-*V* curve not only became more linear, but the magnitude of the *I*-*V* response also increased 20-fold, that is, at  $-10\ \text{V}$ , the magnitude of the current increased from  $-2.1 \times 10^{-5}$  to  $-4.4 \times 10^{-4}\ \text{A}$  (Fig. 9c). Based on these experimental results, we expect that solvent removal will assist in the autonomic restoration of conductivity.

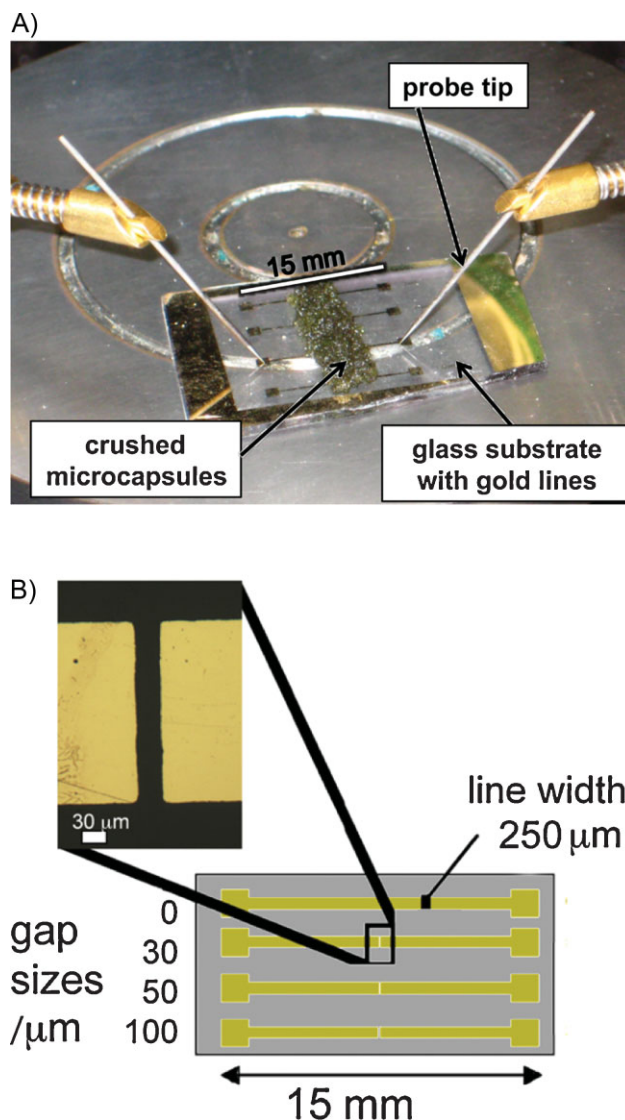


**Figure 8.** A) Photograph of probe station set-up showing crushed microcapsules bridging breaks in gold lines on a glass substrate. B) Pattern design for gold lines with controlled gap sizes on glass substrate optical micrograph of a  $30\ \mu\text{m}$  gap.

### 3. Conclusions

The feasibility of using charge-transfer salt precursors in organic solvents to restore conductivity was demonstrated. Each component of the charge-transfer salt was separately encapsulated as solutions in core-shell microcapsules, and the charge-transfer salt was formed upon combination of the cores of both types of microcapsules after rupture. Both precursor solutions are low viscosity liquids, avoiding delivery problems of viscous solutions or suspensions. This system has the potential to serve as a useful model for a two-part electronic self-healing system using liquid precursors by comparing the degree of restoration of conductivity of one- and two-part microcapsule systems. Investigations are currently underway to study this system in the autonomic healing

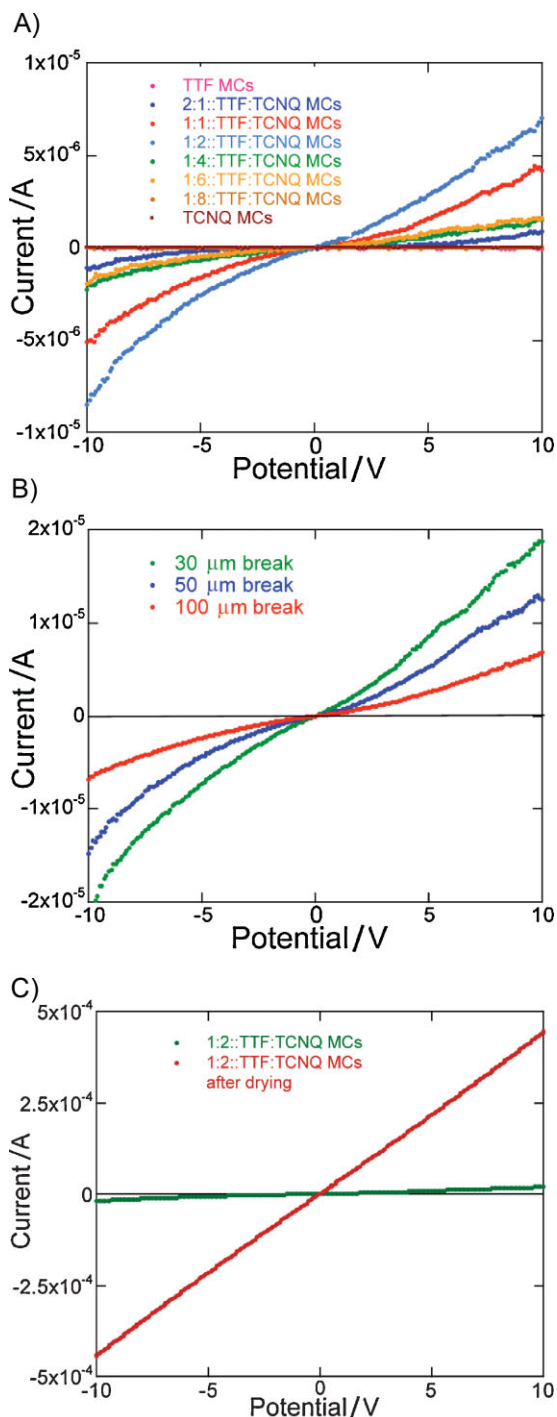


**Figure 9.** A)  $I$ - $V$  measurements for neat ruptured microcapsules on gold line on glass with 50  $\mu\text{m}$  gap, with ratios of MCs noted. B)  $I$ - $V$  measurements for neat ruptured 1:2 TTF:TCNQ MCs deposited onto gold lines on glass with 30, 50, and 100  $\mu\text{m}$  gaps. C)  $I$ - $V$  measurements for neat ruptured 1:2 TTF:TCNQ microcapsules on gold lines with 30  $\mu\text{m}$  gaps immediately after crushing (green) and after drying (red).

of damaged electronic systems, including comparison to alternative, single-capsule systems containing suspensions of conductive materials.

## 4. Experimental

EPA, PA, PhCl, urea, ammonium chloride, and resorcinol were purchased from Aldrich and used as received. TCNQ was purchased from Aldrich and was purified by recrystallization from acetonitrile [32]. For PA-based microcapsules used in electrical measurements, TTF was recrystallized from hexanes as previously described [33]. Ethylene-maleic anhydride copolymer (Zemac-400) powder with an average molecular weight of 400 kDa (Vertellus) was used as a 2.5 wt% aqueous solution. The commercial polyurethane prepolymer Desmodur L 75 was purchased from Bayer MaterialScience and used as received.

Microcapsules were prepared with slight modifications using our previously published procedure [26] in which the shell wall materials and aqueous phase were reduced by half from the initial urea-formaldehyde emulsion procedure [28]. Similarly, 100 mL of deionized water at room temperature was placed in a 600 mL beaker, along with 25 mL of 2.5% (wt/v) ethylene co-maleic anhydride as a surfactant. The beaker was placed in a temperature controlled water bath equipped with a mechanical stirring blade (40 mm diameter), which was brought to 400 RPM. To the aqueous solution was added the solid wall-forming materials: urea (2.50 g), ammonium chloride (0.25 g), and resorcinol (0.25 g). Afterward, the pH was adjusted from 2.7 to 3.5 by addition of aqueous NaOH solution. The core solutions, which were previously sonicated at 40 °C for 30 min to ensure dissolution of the solids, were added to the stirring solution, creating an emulsion. After 10 min, 6.33 g of formalin solution was added and the temperature was increased to 55 °C at 10 °C min<sup>-1</sup>. The reaction proceeded under continuous stirring for 4 h after which the reaction mixture was allowed to cool to room temperature. The microcapsule solution was filtered the next day, washing with water, and then dried under air for at least 6 h before sieving.

For the encapsulation of crystalline TTF-TCNQ, the charge-transfer salt was formed from the combination of TTF in acetonitrile with TCNQ in acetonitrile, then recrystallized from acetonitrile. The crystals were ground such that the length of the longest axis of the majority of the crystals was 100  $\mu\text{m}$  or less. During the encapsulation, the TTF-TCNQ salt was suspended in PA and used as the core material following our previously described procedure for encapsulation [26]. In the case of the encapsulation of powdered TTF-TCNQ, the TTF-TCNQ salt was generated in situ by pouring individual solutions of TTF and TCNQ (0.30 g TTF in 30 mL PA, 0.30 g TCNQ in 30 mL PA, each sonicated at 40 °C for 30 min beforehand) directly into the emulsification polymerization reaction vessel. Higher concentrations of TTF and TCNQ were prepared by adding 3.0 g polyurethane prepolymer to the core solutions before sonication; these microcapsules are labeled TTF-PA\* and TCNQ-PA\*.

Size distributions for capsules prepared were obtained from multiple optical micrographs of dried capsules in mineral oil on glass slides taken using a Leica DMR Optical Microscope at various magnifications (see Supporting Information for size distributions). Capsule diameter measurements were obtained from the micrographs using ImageJ analysis software. A minimum of 100 measurements was used for each analysis of each batch of capsules produced. Microcapsules were sieved to collect those with diameters ranging from 125–180  $\mu\text{m}$ . Images of dried capsules were obtained using SEM (FEI/Philips XL30 ESEM-FEG) after sputter coating with a gold-palladium source.

TGA was performed on a Mettler-Toledo TGA851, calibrated by indium, aluminum, and zinc standards. A heating rate of 10 °C · min<sup>-1</sup> was used, and experiments were performed under nitrogen atmosphere from 25–650 °C. For each experiment, approximately 5 mg of sample were accurately weighed ( $\pm 0.02$  mg) into an alumina crucible.

Mass spectra were recorded on a 70-VSE C in EI+ mode through the University of Illinois Mass Spectrometry Laboratory, SCS. The samples were obtained by crushing microcapsules with a mortar and pestle. The residues were dried under vacuum for ca. 24 h (120 mTorr) to remove the

majority of the core solvent. Samples of the remaining core and shell wall were submitted for mass spectroscopy.

Elemental analyses were performed by the University of Illinois Microanalysis Laboratory. Samples of microcapsule shell walls were prepared by crushing the microcapsules with a mortar and pestle, then washing the shell walls with dichloromethane and collecting the walls with a Büchner funnel. The shell walls were dried at room temperature (ca. 22 °C) under vacuum (120 mTorr) for one week before submission for elemental analysis.

Absorption spectra were recorded using a Shimadzu UV-vis Spectrophotometer, model number UV-1601PC. Before analysis, all microcapsule samples were soaked for 5 min in dichloromethane, then were rinsed with dichloromethane to remove any TTF or TCNQ from the microcapsule surface. For soaking experiments, the microcapsules of known masses (generally 50–100 mg) were immersed in a known volume of dichloromethane (generally 2–5 mL). The samples were then filtered gently using syringe filtration (pore diameter 45 µm). UV-vis absorption spectra were recorded of the filtered solutions.

For absorption spectra of ruptured microcapsules, a known mass of microcapsules (generally 50–100 mg) was ruptured by grinding in a mortar and pestle. The slurry of ruptured microcapsules was transferred to a vial using a known volume of solvent (generally 2–5 mL), and the suspension was filtered to remove the shell wall. The absorption spectra of the filtered solution was recorded, which was further diluted quantitatively to obtain absorbance values between 0.5–1.5.

Powder XRD measurements were performed on neat crushed microcapsules, dried versions thereof, or precipitates from the microcapsule cores using a Bruker General Area Detector Diffraction System.

I–V measurements were performed using a two-point measurement technique at a Signatone table-top probe station customized with a standard S725 manipulator. Tungsten probe tips were immersed in suspensions of microcapsules (crushed by mortar and pestle) approximately 100 µm apart. The voltage was swept from –10 to +10 V continuously 5–7 times for each sample using an Agilent 4155C Semiconductor Parameter Analyzer.

Substrates for conductivity measurements were prepared as follows. Glass slides were cleaned using Piranha solution (3:1 v/v conc. H<sub>2</sub>SO<sub>4</sub>:30% H<sub>2</sub>O<sub>2</sub>) for 1 h and then rinsed with Milli-Q water (>18 MΩ·cm) and dried under a stream of nitrogen. Shipley 1805 was spin-coated onto the cleaned wafers at 3000 RPM for 30 s. The photoresist was patterned through a transparency mask using a Karl Suss mask aligner (~16 mW cm<sup>-2</sup>) for 10 s. After development of the photoresist using AZ 351 developer, a 10 nm chromium adhesion layer followed by a 50 nm Au layer was deposited by electron beam evaporation. Sonication of the substrates in acetone removed any remaining photoresist and gold overlayer. Gold gate dimensions were confirmed by optical microscopy.

## Acknowledgements

This work was partially supported by the National Science Foundation for funding through a National Science and Engineering Initiative (Award Number DMR-0642573). Additionally, funding for electrical measurements and device fabrication was supported by the Center for Electrical Energy Storage, an Energy Frontier Research Center funded by the U.S. Department of Energy, Office of Science, Office of Basic Energy Sciences. S. Odom thanks the National Science Foundation for an American Competitiveness in Chemistry Fellowship funded by the American Recovery and Reinvestment Act. M. Caruso thanks the Department of Defense for an NDSEG Fellowship. We thank Audrey Bowen for assistance with photolithography, Scott Robinson in the Imaging Technology Group at the Beckman Institute for assistance with SEM imaging, and Danielle Gray for powder XRD collection and analysis. We also thank Vertellus for their donation of Zamac-400. Supporting Information is available online from Wiley InterScience or from the author.

Received: January 27, 2010  
Published online: May 3, 2010

- [1] M. L. Minges, *Electronic Materials Handbook: Packaging*, ASM International, Handbook Committee, 1989.
- [2] A. W. Sleight, *Endeavour* 1995, 19, 64.
- [3] M. Ohring, *Reliability and Failure of Electronic Materials and Devices*, Academic Press, San Diego 1998.
- [4] M. Zhao, L. Jiao, H. Yuan, Y. Feng, M. Zhang, *Solid State Ionics* 2007, 178, 387.
- [5] R. B. R. van Silfhout, Y. Li, W. D. van Driel, *Proc. EuroSIME* (Ed.: L. J. Ernst), Shaker Publishing BV, Maastricht 2001, pp. 207–301.
- [6] P. Viswanadham, P. Singh, *Failure Modes and Mechanisms in Electronic Packages*, Chapman & Hall, New York 1998.
- [7] K. A. Williams, A. J. Boydston, C. W. Bielawski, *J. R. Soc. Interface* 2007, 4, 359.
- [8] M. M. Caruso, S. R. Schelkopf, A. C. Jackson, A. M. Landry, P. V. Braun, J. S. Moore, *J. Mater. Chem.* 2009, 19, 6093.
- [9] M. M. Caruso, D. A. Davis, Q. Shen, S. A. Odom, N. R. Sottos, S. R. White, J. S. Moore, *Chem. Rev.* 2009, 109, 5755.
- [10] S. R. White, N. R. Sottos, P. H. Geubelle, J. S. Moore, M. R. Kessler, S. R. Sriram, E. N. Brown, S. Viswanathan, *Nature* 2001, 409, 794.
- [11] S. H. Cho, H. M. Andersson, S. R. White, N. R. Sottos, P. V. Braun, *Adv. Mater.* 2006, 18, 997.
- [12] J. M. Kamphaus, J. D. Rule, J. S. Moore, N. R. Sottos, S. R. White, *JRS Interface* 2008, 5, 95.
- [13] S. R. White, M. M. Caruso, J. S. Moore, *MRS Bull.* 2008, 33, 766.
- [14] L. B. Coleman, M. J. Cohen, D. J. Sandman, F. G. Yamagishi, A. F. Garito, A. J. Heeger, *Solid State Commun.* 1973, 12, 1125.
- [15] J. Ferraris, D. O. Cowan, V. Walatka, J. H. Perlstein, *J. Am. Chem. Soc.* 1973, 95, 948.
- [16] S. M. Rosenfeld, R. G. Lawler, H. R. Ward, *J. Am. Chem. Soc.* 1973, 95, 946.
- [17] D. Jérôme, *Chem. Rev.* 2004, 104, 5565.
- [18] E. M. E. Conwell, *Semiconductors and Semimetals, Highly Conductive Quasi-One Dimensional Organic Crystals*, Vol. 27, Academic Press, London 1998.
- [19] Y. Takahashi, T. Hasegawa, Y. Abe, Y. Tokura, G. Saito, *Appl. Phys. Lett.* 2006, 88, 073504.
- [20] Y. Takahashi, T. Hasegawa, S. Horiuchi, R. Kumai, Y. Tokura, G. Saito, *Chem. Mater.* 2007, 19, 6382.
- [21] H. Wada, T. Taguchi, B. Noda, T. Kambayashi, T. Mori, K. Ishikawa, H. Takezoe, *Org. Electron.* 2007, 8, 759.
- [22] A. Figueras, J. Caro, J. Fraxedas, V. Laukhin, *Synth. Met.* 1999, 102, 1611.
- [23] K. Yase, N. Ara, A. Kawazu, *Mol. Cryst. Liq. Cryst.* 1994, 247, 185.
- [24] M. Hiraoka, T. Hasegawa, T. Yamada, Y. Takahashi, S. Horiuchi, Y. Tokura, *Adv. Mater.* 2007, 19, 3248.
- [25] T. Sumimoto, K. Kudo, T. Nagashima, S. Kuniyoshi, K. Tanaka, *Synth. Met.* 1995, 70, 1251.
- [26] B. J. Blaiszik, M. M. Caruso, D. A. McIlroy, J. S. Moore, S. R. White, N. R. Sottos, *Polymer* 2009, 50, 990.
- [27] M. M. Caruso, B. J. Blaiszik, S. R. White, N. R. Sottos, J. S. Moore, *Adv. Funct. Mater.* 2008, 18, 1898.
- [28] E. N. Brown, M. R. Kessler, N. R. Sottos, S. R. White, *J. Microencapsulation* 2003, 20, 719.
- [29] M. M. Caruso, B. J. Blaiszik, H. Jin, S. R. Schelkopf, D. S. Stradley, N. R. Sottos, S. R. White, J. S. Moore, *ACS Appl. Mater. Interfaces* 2010, in press.
- [30] L. R. Melby, R. J. Harder, W. R. Hertler, W. Mahler, R. E. Benson, W. E. Moche, *J. Am. Chem. Soc.* 1962, 84, 3374.
- [31] T. Tomkiewicz, J. B. Torrance, B. A. Scott, D. C. Geen, *J. Chem. Phys.* 1974, 60, 5111.
- [32] W. L. F. Armarego, C. L. L. Chai, *Purification of Laboratory Chemicals*, 5th ed. Butterworth Heinemann, Elsevier Science, Oxford 2003.
- [33] R. McIntyre, H. Gerisher, *Ber. Bunsen-Ges.* 1984, 88, 963.